Heliyon 10 (2024) e28971

Contents lists available at ScienceDirect

Heliyon

journal homepage: www.cell.com/heliyon

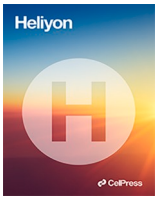

Research article

Penicillium polonicum-mediated green synthesis of silver nanoparticles: Unveiling antimicrobial and seed germination advancements

Yunhao Zhu [a,b,1], Xiangxiang Hu [a,1], Mengyi Qiao [a], Le Zhao [a], Chengming Dong [a,b,*]

[a] *School of Pharmacy, Henan University of Chinese Medicine, Zhengzhou, Henan, PR China*
[b] *Co-construction Collaborative Innovation Center for Chinese Medicine and Respiratory Diseases by Henan & Education Ministry of PR China, PR China*

ARTICLE INFO

Keywords:
Silver nanoparticles
Fungus
Green synthesis
Antimicrobial activity
Seed germination

ABSTRACT

Silver nanoparticles (AgNPs), widely recognized for their nanoscale geometric size and unique properties, such as large specific surface area, high permeability, and high safety, were synthesized using the endophytic fungus *Penicillium polonicum* PG21 through a green approach. Four key synthesis factors—48 h, 45 °C, pH 9.0, and 80 mM AgNPs concentration—were optimized. Characterization via ultraviolet–visible spectroscopy, transmission electron microscopy, Fourier-transform infrared spectroscopy, and X-ray diffraction revealed the AgNPs as approximately 3–25 nm spherical particles with numerous functional groups ensuring stability. AgNPs were tested against various fungal and bacterial plant pathogens, including *Botrytis cinerea* (EB-1), *Alternaria alternata* (EB-2, EB-3), *Fusarium solani* (RG-1), *Williamsia serinedens* (SL-1), *Sphingopyxis macrogoltabida* (SL-2), *Bacillus velezensis* (SL-3), and *Pseudomonas mediterranea* (SL-4), causing agricultural challenges. PG21-synthesized AgNPs exhibited inhibition rates against all tested fungi, with 60 μg/mL AgNPs demonstrating optimal inhibition rates. Notably, EB-1 experienced a significant growth inhibition, reaching an inhibition rate reached of 74.22 ± 1.54%. Conversely, RG-1 exhibited the smallest inhibitory effect at 48.13 ± 0.92%. The effect of AgNPs on safflower seed germination and growth revealed notable increases in shoot length, fresh weight, stem length, and number of lateral roots—1.4, 1.4, 1.33, and 10.67 times higher than the control, respectively, at an AgNPs concentration of 80 μg/mL. In conclusion, green-synthesized AgNPs demonstrate pathogen toxicity, showcasing potential applications in disease management for industrial crops and promoting plant growth.

1. Introduction

Nanotechnology, a rapidly advancing field, offers numerous implications for various aspects of human life. Nanoparticles (NPs), owing to their diminutive size, are extensively used in photocatalysis [1,2], photoelectric sensing [3,4], environmental science [5,6], biomedicine [7], and other fields. Their ability to transverse cell walls enables direct impact on plants, animals, and various microorganisms. Among the widely employed NPs, AgNPs possess crucial properties such as disease resistance, sterilization, plant growth

* Corresponding authorJinshui East Road No.156, Zhengzhou, Henan, 450046, PR China.
E-mail address: dcm371@sohu.com (C. Dong).
[1] These authors contributed equally to this work.

https://doi.org/10.1016/j.heliyon.2024.e28971
Received 6 December 2023; Received in revised form 1 March 2024; Accepted 27 March 2024
Available online 4 April 2024

promotion, antioxidant activity, and antibacterial effects [8]. The exceptional antimicrobial activity of AgNPs arises from their ability to disrupt cell walls and membranes, induce nucleic acid damage, and generate reactive oxygen species (ROS) [9,10].

A previous study highlighted the antibacterial effect of silver ions [11], demonstrating that AgNPs effectively reduced sclerotia-forming fungi in a dose-dependent manner [12]. Agriculture can also benefit from AgNPs, with AgNPs at appropriate concentrations significantly promoting seed germination. In tulip plants, AgNPs increased the leaf greenness index, stomatal conductance, fresh root weight, and root length [13]. In *Lavandula angustifolia* [14], AgNPs addition to the culture medium increased shoot formation and fresh weight. Furthermore, AgNPs improved seed germination in tomato plants [15].

AgNPs are currently synthesized chemically, physically, and biologically [16]. Chemical and physical methods, known for their harsh conditions leading to environmental pollution, yield low and require high energy consumption. From the perspective of green chemistry, microorganisms are regarded as "green factories" for NP production [17,18]. Fungi produce numerous metabolites, rendering them more suitable for NPs production [19]. Several studies have confirmed the capability of *Aspergillus*, *Penicillium*, and *Fusarium* to synthesize AgNPs [20,21].

Rehmannia glutinosa Libosch and *Epimedium sagittatum* (Sieb. et Zucc.) Maxim are widely used in traditional Chinese medicine (TCM) [22]. Ring rot, caused by RG-1, poses a severe threat to *R. glutinosa* cultivation by damaging plant leaves and significantly affecting both yield and quality [23]. Leaf blight and grey mold, primarily caused by EB-1, EB-2, and EB-3, are two major diseases affecting *E. sagittatum*. A grey mold outbreak can result in a 2.35% plant loss and 15.27% diseased plants, whereas leaf blight outbreaks can result in a 4.08% plant loss and 17.96% diseased plants.Tomatoes, globally significant for their economic and nutritional value, are extensively cultivated in southern and northern China [24]. Pathogenic bacteria affecting tomatoes include SL-1, SL-2, SL-3, and SL-4. This study utilized *P. polonicum* PG21 to synthesize AgNPs with a diameter of 10 nm, aiming for environmentally friendly prevention and control in industrial crops such as *R. glutinosa* and *E. sagittatum*. The synthesized AgNPs effectively inhibited pathogens *in vitro*, suggesting broad-spectrum resistance to both fungal and bacterial pathogens and providing new insights into future disease control in industrial crops.

Additionally, the role of AgNPs was further explored in safflower (*Carthamus tinctorius* L.) seed germination. Results showed a significant increase in shoot length, fresh weight, stem length, and the number of lateral roots in safflower seeds with 80 μg/mL AgNPs compared to the control group, supporting the theoretical application of AgNPs as seed germination promoters. Furthermore, endophytic fungi capable of biosynthesizing AgNPs were screened and identified. This analysis helped determine optimal synthesis conditions through parameter optimization and evaluate the antimicrobial activity of the resulting AgNPs and their effect on plant growth and development.

The aim of this study was to screen and identify endophytic fungi capable of biosynthesising AgNPs, to determine the optimal synthesis conditions by optimising the synthesis parameters, and to test the antimicrobial activity of the resulting AgNPs as well as their effect on plant growth and development.

2. Materials and methods

2.1. Strains and materials

Selected fungi were cultivated on a potato-sucrose-agar (PSA) slant [25]. *P. polonicum* was isolated from surface-sterilised leaves of *R. glutinosa*. *R. glutinosa* leaves were cut into segments of approximately 0.5 × 0.5 cm^2, immersed in 75% ethanol for 30 s, washed in sterile water 3–4 times, immersed in sterile water 3–4 times, immersed in 0.1% mercuric chloride for 10–15 min, and again washed in sterile water 6–8 times. Disinfected leaves were placed on PSA medium and incubated in a 28 °C incubator.The antimicrobial efficacy of AgNPs was assessed against four pathogenic fungi and bacteria. Specifically, the fungi (EB-1, EB-2, and EB-3 from *R. glutinosa* and RG-1 from *R. glutinosa*) were previously isolated and preserved in the laboratory, while the bacteria (SL-1, SL-2, SL-3, and SL-4), all tomato pathogens, and contributed by Prof Xu Kedong of Henan Key Laboratory of Crop Molecular Breeding and Bioreactor.

2.2. Morphology and molecular identification

The strain for AgNP synthesis was isolated from *R. glutinosa*, cultured on PSA at 28 °C, and preserved at 4 °C. Colony morphology was examined by growing it on PSA medium at 28 °C for 4–5 d, followed by observing spore and mycelium morphology using an optical microscope. Fungi were then grown in 50 mL PSA liquid medium at 28 °C for 7 d. DNA was extracted using the Ezup Column Fungi Genomic DNA Purification Kit. PCR was used to amplify the fungal internal transcribed spacer (ITS), β-tubulin (BenA), and calmodulin (CaM) regions [26,27].The primer sequences are shown in Table 1.

Table 1
Primers used for the amplification of specific genes in the fungal isolates.

Gene name	Oligonucleotide sequence (5′–3′)	Length (bp)	Annealing temperature (°C)
ITS	TCC GTA GAA CCT GCC G TCC TCC GCT TGA TAT GC	600	55.1
BenA	GGT AAC CAA ATC GGT GCT GCT TTC ACC CTC AGT GTA GTG ACC CTT GGC	500	60
CaM	CCG AGT ACA AGG ARG CCT TC	580	57

PCR reactions consisted of a 20 μL mixture: 1 μL DNA template, 1 μL each of forward and reverse primers, 10 μL 2 × PCR Master Mix (2 × Taq DNA Polymerase, 2 × PCR Buffer, 2 × dNTP), and sterile double-distilled water to reach a final volume of 20 μL.

For homology studies, sequencing results were compared with other sequenced *Penicillium* strains using BLASTN on Ensemble. The access numbers for *Penicillium polonicum* were PP112154 (ITS); PP130078 (BenA); PP130079 (CaM).The MEGA v7.0 software was used to generate different phylogenetic trees using the neighbor-joining method, based on 1000 replicates of guide values, with *Aspergill awamori str. IFM 58123* used as the out-group.

2.3. AgNPs biosynthesis

The 10 mm fungal blocks were inoculated into a PSA liquid medium and cultured on a constant temperature shaker at 28 °C and 120 rpm for 7 d. Subsequently, the wet biomass was filtered and washed 4–5 times with double-distilled water to eliminate the medium. An appropriate amount of wet biomass was added to a flask containing 50 mL of double-distilled water. This mixture was incubated at 28 °C for 24 h under shaking conditions (120 rpm/min). The biomass filtrate was subsequently mixed with a 9:1 solution of 10 mM silver nitrate ($AgNO_3$) at 28 °C for 24 h in the dark. The silver ions were reduced to metallic silver, resulting in the synthesis of AgNPs. The final reaction sample was collected and centrifuged at 10,000 rpm for 30 min to generate pellets for subsequent experiments [28,29].

2.4. Optimization of AgNPs biosynthesis

Four key factors influencing AgNPs synthesis were investigated: substrate $AgNO_3$ concentration (5, 10, 20, 40, 80 and 160 mM), temperature (4, 28, 37, 45 °C), pH (4, 5, 6, 7, 8, 9, and 10), and incubation time (12, 24, 48, and 60 h). After reactions under each condition, 3 mL of the sample was extracted and analyzed using a UV spectrophotometer.

2.5. Characterization of AgNPs

Ultraviolet–visible (UV–Vis) spectrum: The initial indicator for AgNPs detection is the color change in the reaction solution and $AgNO_3$ solution. Characteristic peaks UV–Vis spectroscopy with a wavelength range of 300–800, with a resolution of 1 nm.

Transmission electron microscopy (TEM): The size distribution and morphology of AgNPs were examined using TEM at an 80 KV voltage. Samples were prepared by placing a 10 μL aliquot of biogenic AgNPs on carbon-coated copper grids [30].

Fourier-transform infrared spectroscopy (FTIR): Functional groups on the surface of AgNPs were characterized using FTIR spectroscopy. Dry nanosilver powder was measured, and a mixture with potassium bromide (KBr) at a 1:200 ratio was tableted. Spectra were scanned in the 400–4000 cm^{-1} range at a resolution of 4 cm.

X-ray diffraction (XRD): Structural analysis of biogenic AgNPs was conducted using XRD with Cu Kα radiation ($\lambda = 0.15418$ nm) across the scanning range $2\theta = 5$–90°, and the scanning speed was set at 10°/min [31].

2.6. Antifungal activity of AgNPs

The antifungal activity of AgNPs was evaluated using the mycelial growth rate method. The initial AgNP concentration was 1.0×10^4 μg/mL, and various working concentrations (10, 20, 30, 40, 50, and 60 μg/mL) were prepared by diluting the original stock solution with distilled water, which was then mixed with the PSA medium [32]. After solidifying the medium, uniform-sized agar plugs (diameter, 10 mm) containing fungi were simultaneously inoculated into the center of each Petri dish containing AgNPs, followed by incubation at 28 °C for 7 d. The growth inhibition rate of hyphae was calculated using the cross-bonded method, with the following formula used to calculate the inhibition rate (%) [33]:

$$\text{Inhibition rate } (\%) = \frac{R - r}{R - A}$$

where R represents the growth of fungal mycelia on the control plate, r represents the growth of fungal mycelia on the plate treated with AgNPs, and A represents the size of the agar block.

2.7. Antibacterial activity of AgNPs

In this experiment, the antibacterial activity of AgNPs was investigated by means of a simple, practical and highly standardised Oxford cup method [34]. AgNPs were dissolved in sterile distilled water to create a 1.0×10^4 μg/mL solution. Using a standard 0.5 McFarland suspension, the concentration of pathogenic bacteria was assessed after overnight incubation in Luria–Bertani (LB) medium, resulting in a 1.0×10^6 CFU [35]. For each plate with 30 mL of sterile LB medium, 100 μL of the bacterial solution was inoculated. Distilled water was used as the negative control, and ampicillin as the positive control. Plates were incubated at a constant temperature of 37 °C for 15 h to determine the size of the inhibition zone, with each treatment replicated three times.

The minimum inhibitory concentration (MIC), defined as the lowest antimicrobial concentration inhibiting visible growth, and minimum biocidal concentration (MBC), representing the lowest concentration killing ≥99.9% of the cells, were determined in a 96-well microplate using the microdilution method [36]. The bacterial solution was mixed with AgNPs, resulting in a final AgNP

concentration range of 512–0 μg/mL, and cultured overnight at 28 °C. The turbidity of the well mixture was measured and recorded. After incubation, 50 μL from each clarified well was transferred to LB agar for bacterial culture and incubated at 37 °C for 15 h.

2.8. Seed growth and development

Seeds of uniform size and full particles were randomly selected and soaked in AgNPs solutions (10, 20, 40, 80, and 160 μg/mL in water) for 8 h. Germination was evaluated in an artificial incubator set at 85% relative humidity, with a 16 h light/8 h dark photoperiod and 8000 lx irradiance. Fresh weight, bud length, number of lateral roots, and stem length were measured after 10 d.

2.9. Statistical analysis

Data are expressed as mean ± standard deviation. Data from various treatments were statistically analyzed using the *t*-test, with a significance level set at 0.5.

3. Results

3.1. Screening of strains with AgNPs synthesis potential

Among the 67 strains of endophytic fungi from *R. glutinosa*, 13 exhibited the ability to synthesize AgNPs, with PG21 demonstrating the highest ability. (Supplementary Table 1).

3.2. Morphological and molecular characterization

3.2.1. Morphological characterization

Upon examination of its colony morphological characteristics (Fig. 1a), which include an overall cyan-green color, powdery texture, and a white rim, along with microscopic features of broom-like conidiophores (Fig. 1b), the strain was identified as a *Penicillium* member.

3.2.2. Molecular characterization

PCR amplification of the strain's genome, focusing on ITS, BenA, and CaM sequences, resulted in 400–600 bp-sized amplicons. The phylogenetic trees of the fungal isolates revealed that strain PG21 clustered on the same branch as *P. polonicum*, suggesting a close genetic relationship. Fig. 1c depicts the phylogenetic relationship between the fungal strain utilized in AgNPs biosynthesis and closely related strains obtained from *EnsemblFungi* (http://fungi.ensembl.org/index.html).

3.3. AgNPs biosynthesis

AgNPs were synthesized in the dark at 28 °C. The addition of 10 mM $AgNO_3$ to the PG21 secondary fermentation broth induced a color change in the medium. After 24 h, the $AgNO_3$-treated fermentation broth exhibited a brown color (Fig. 3a). Conversely, the positive control, incubated with double deionized distilled water, retained its original color due to surface plasmon resonance (SPR) of

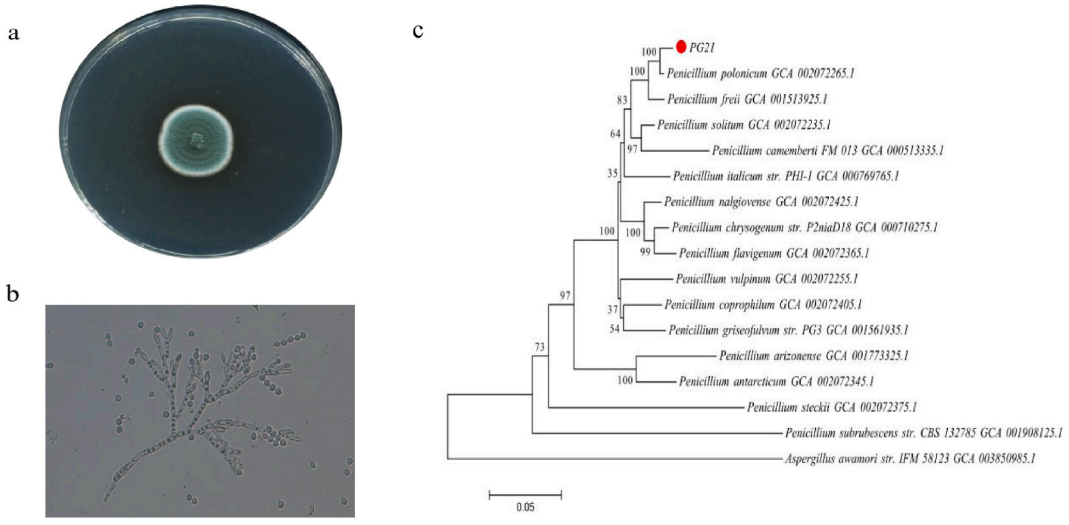

Fig. 1. Identification of endophytic fungus PG21 (a) colony morphology, (b) Mycelium and spore morphology, and (c) phylogenetic tree.

AgNPs.

3.4. Optimization of AgNPs biosynthesis

The investigation into cultivation conditions, including temperature, pH, substrate concentration, and reaction time, revealed the factors affecting AgNPs production from PG21 biomass filtrate.

3.4.1. Effects of reaction temperature profile on AgNPs formation

Examining the effect of incubation temperature on the biosynthetic ability of AgNPs in the biomass filtrate (Fig. 2a) revealed an increasing absorbance peak with rising temperatures from 4 °C to 45 °C. The optimum reaction temperature, producing the most efficient reduction filtrate and the highest AgNPs yield, was identified as 45 °C with an absorption peak at 445 nm.

3.4.2. Effects of reaction media pH on AgNPs formation

Different strains require different pH environments for AgNPs synthesis. The effect of pH on the ability of PG21 to synthesize AgNPs was investigated. The biomass filtrate from PG21 grown at pH 9.0 displayed a preference for AgNPs formation. At pH 11.0, the absorption peak red-shifted, causing an increase in the synthesized AgNPs particle size. The absorbance curve of AgNPs prepared through the biomass filtrate grown in a pH 9.0 medium revealed an absorbance peak at 431 nm (Fig. 2b). Other biomass filtrates from mycelial biomass collected at pH 7.0 and 8.0 also supported AgNPs formation but to a lesser extent.

3.4.3. Effect of substrate concentration on AgNPs formation

The investigation into the effects of different $AgNO_3$ concentrations on AgNPs synthesis revealed that the optimum substrate concentration was 80 mM (Fig. 2c). This finding suggests that maintaining synthesis conditions at this concentration is crucial for optimal results.

3.4.4. Effect of reaction time on AgNPs formation

A maximum absorption peak was observed at 450 nm when the reaction time was 60 h (Fig. 2d). However, a shift occurred from 60 to 48 h, causing a blue shift and decreasing the particle size of the synthesized AgNPs.

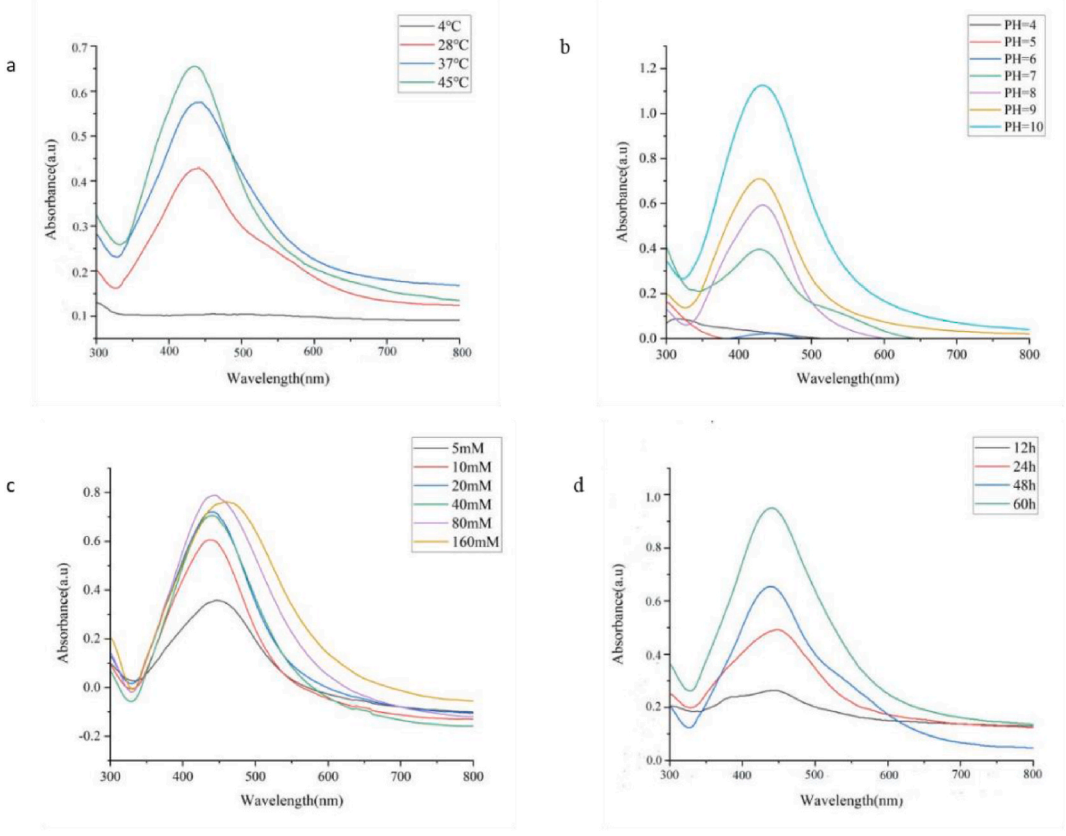

Fig. 2. UV–vis absorption spectra of AgNPs synthesized at different conditions (a) temperature, (b) pH, (c) AgNO3 concentrations, and (d) reaction time.

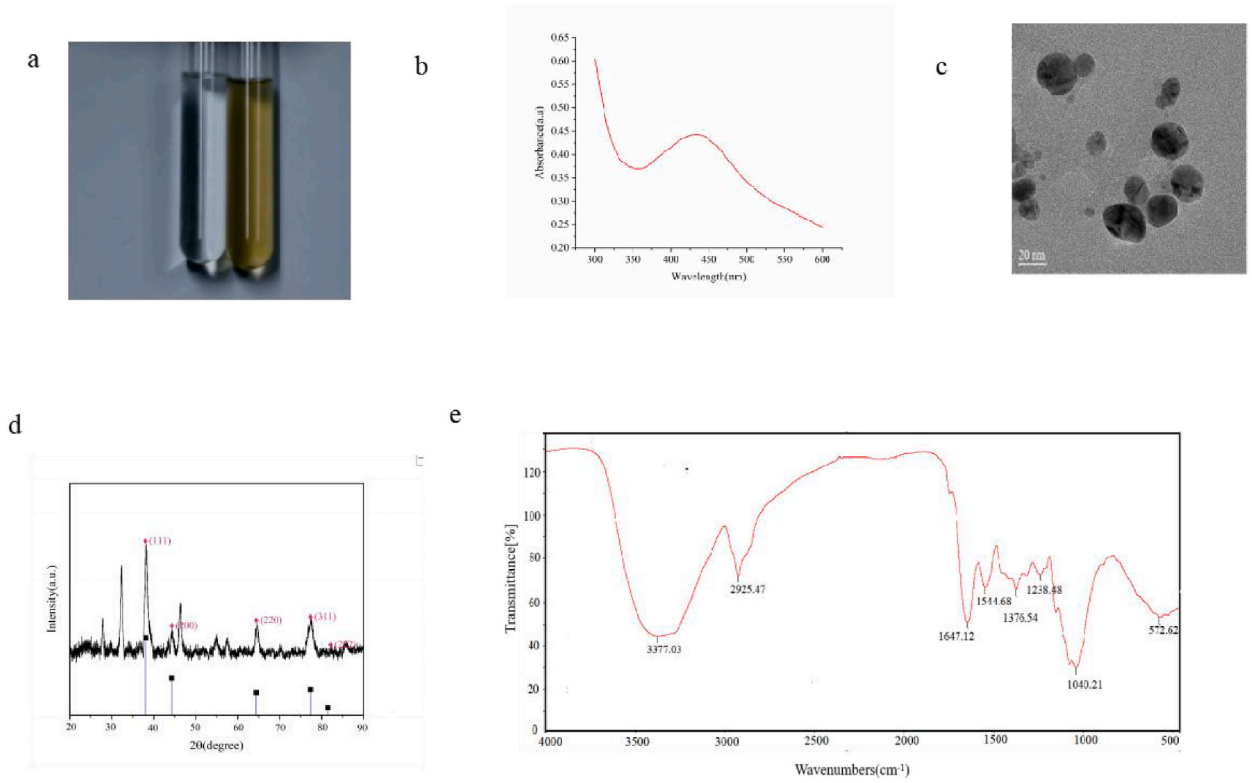

Fig. 3. Characterization of the AgNPs synthesized by Penicillium polonicum PG21 (a) Colour change of the reaction, (b) UV–vis absorption spectrum, (c) TEM image, (d)XRD pattern, and (e) FTIR spectra.

These findings highlight the diverse factors influencing AgNPs synthesis, requiring optimization to achieve the optimal synthesis state. The identified optimal conditions for AgNPs biosynthesis were 45 °C, pH 9.0, 48 h, and an 80 mM substrate concentration.

3.5. AgNPs characterization

The reaction mixture was incubated overnight and evaluated using a UV–Vis spectrophotometer, revealing a characteristic peak near 400–450 nm, confirming the formation of AgNPs (Fig. 3b).

The shape and size of the synthesized AgNPs were observed through TEM, indicating a spherical or nearly spherical shape with particle size range of 3–25 nm (Fig. 3c).

XRD analysis revealed the crystalline nature of the physiologically produced AgNPs (Fig. 3d). In the spectrum of 2θ value ranging from 5° to 90°, peaks at 38.11°, 44.30°, 64.44°, and 77.40°, corresponding to (111), (200), (220), and (311) planes, respectively, aligned with standard XRD data for elemental silver (JCPDS File No. 04–0783).

FTIR analysis (Fig. 3e) revealed the biological functional groups involved in AgNPs preparation. Absorption peaks at 3377.03, 2925.47, 1647.12, 1376.54, and 1040.21 cm^{-1} indicated various functional groups. The strong, broad adsorption band at 3377.03 cm^{-1} suggested O–H stretching vibrations of benzene or phenols. Peaks around 2925 cm^{-1} corresponded to–CH_2 stretching vibrations. An additional peak between 1400 and 1550 cm^{-1} indicated the presence of N–H aromatic secondary amine, attributed to the N–H stretching in the synthesized AgNPs. The strong adsorption band at 1600–1650 cm^{-1}, attributed to the carbonyl stretching in the

Table 2
Inhibition rate (%) and EC_{50} (%) of AgNPs against plant pathogenic fungi *in vitro*.

Isolate	Inhibition rates (%)							EC50 (μg/ml)
	0	10 μg/mL	20 μg/mL	30 μg/mL	40 μg/mL	50 μg/mL	60 μg/mL	
EB-1	–	1.55 ± 0.39	26.45 ± 0.39	48.22 ± 1.39	52.45 ± 0.39	67.11 ± 0.77	74.22 ± 1.54	10.31 ± 0.34
EB-2	–	2.78 ± 0.69	23.41 ± 0.69	32.53 ± 1.37	36.51 ± 1.38	37.69 ± 0.69	54.36 ± 1.82	7.60 ± 0.39
EB-3	–	2.80 ± 0.80	12.96 ± 0.80	18.06 ± 1.39	31.02 ± 0.80	38.89 ± 1.39	63.43 ± 0.80	7.91 ± 0.50
RG-1	–	6.36 ± 0.91	24.24 ± 1.05	31.82 ± 1.58	49.09 ± 1.82	47.57 ± 0.53	48.13 ± 0.92	5.36 ± 1.05

Inhibition rates were determined based on three replicates of each experiment, "-" means the inhibition rate is 0.The mean and standard deviation (SD) reported for each microbial strain were based on three biological replicates.

protein's C═O group, suggested the presence of proteins or other compounds on the AgNP surface, contributing to stability and preventing agglomeration [37].

3.6. Antifungal activity of fungi

The inhibitory effect of different AgNPs concentrations on PSA was assessed, with the most significant inhibition observed at a concentration of 60 μg/mL (Table 2). As AgNPs concentrations increased, the inhibitory effect on EB-1 and EB-3 became more pronounced, with inhibition rates of EB-1 and EB-3 exceeding 60% at 60 μg/mL. Conversely, RG-1 and EB-2 showed significantly less inhibition compared to other fungi. The EC_{50} values obtained from non-linear fitting indicated the order of virulence as RG-1 > EB-2 > EB-3 > EB-1, with RG-1 exhibiting the highest toxicity. The nonlinear fitting results were plotted in S-Fig. 1 (Supplementary)

3.7. Antibacterial activity of bacteria

Table 3 illustrates the inhibition zone diameters produced by AgNPs on the four tested bacteria. Variations in inhibition zone diameters indicated varying sensitivity of the bacteria to AgNPs. SL-3 showed the highest sensitivity, forming an inhibition zone of 16.8 ± 0.76 mm, followed by SL-1, with an inhibition zone of 16.17 ± 0.29 mm. Conversely, SL-4 was the least sensitive. The inhibition zone diameter of AgNPs against SL-2 was 10.67 ± 0.29 mm, slightly larger than that of SL-4.

The MIC values, ranging from 16 to 32 μg/mL, indicate inhibition of most tested bacteria at 32 μg/mL. SL-1, SL-2, and SL-3 had MIC values of 32 μg/mL, whereas SL-4 had a lower MIC of 16 μg/mL.

The mixed liquid in the clarified tube was placed on the LB solid plate and incubated overnight at 28 °C. Subsequent colony growth is documented in Table 3. The MBC varied from 32 to 128 μg/mL for the seven tested bacteria. SL-1 exhibited the highest resistance, necessitating 128 μg/mL AgNPs for irreversible effects that led to death.

3.8. Seed germination

Soaking seeds in various concentrations of AgNPs demonstrated improvement in the seedling growth index, with the treatment group outperforming the control group in terms of lateral root number, stem length, fresh weight, and bud length in Fig. 4a-d (P10: 10 μg/mL; P20: 20 μg/mL; P40: 40 μg/mL; P80: 80 μg/mL; P160: 160 μg/mL). In particular, the P40 treatment group exhibited 10.67 times more lateral roots than the control group, a statistically significant difference ($P < 0.0001$) across different AgNP concentrations. However, beyond a concentration of 160 μg/mL, safflower growth was no longer promoted, and the indices were lower than those of the P80 group. And the root length, fresh weight, stem length and number of lateral roots were 1, 4, 1.4, 1.33 and 1.67 times higher than the control. Consequently, we hypothesized that within a specific concentration range, applying an AgNPs solution significantly promotes safflower seed germination and growth, whereas a higher AgNPs concentration has no significant effect on its growth.

4. Discussion

Nanoparticle biosynthesis, a green chemical method integrating nanotechnology and microbial biotechnology, offers an environmentally friendly and pollution-free approach to synthesizing AgNPs, significantly lowering the cost. Biosynthesis presents distinct advantages over chemical and physical methods, involving the reduction of silver ions with biologically active microbial fermentation broth to produce AgNPs with controlled size and morphology. The bacterial liquid acts as both a reducing agent and stabilizer, eliminating the need for surfactants, protective agents, or cross-linking agents during the reduction process. Previous studies have highlighted the biosynthesis of AgNPs by fungi such as *Fusarium* [39], *Aspergillus* [40,41], and *Penicillium* [42,43]. For instance, *Fusarium oxysporum* synthesized AgNPs of 5–15 nm in an aqueous Ag + solution [44,45].

In this study, AgNPs were biosynthesized using the endophytic fungus PG21, isolated from the root tube of *R. glutinosa* in Henan Province, China. Morphological and molecular biological methods confirmed its identification as *P. polonicum*. The antimicrobial efficacy of the synthesized AgNPs was evaluated against eight plant pathogen strains, demonstrating notable activity against various pathogens [46,47]. Moreover, AgNPs could promote safflower seed germination and growth. The antimicrobial potency of AgNPs, synthesized from the fungal fermentation broth, was particularly robust, leading to a deceleration in pathogen growth with increasing AgNPs concentration [48]. Additionally, the diameter of pathogenic fungal colonies decreased with increasing concentration [49].

Table 3
Mean zone of inhibition (mm) and antimicrobial activity (MIC and MBC values in μg/ml) of AgNPs against SL-1、SL-2、SL-3 and SL-4.

Bacteria strains	AgNPs (μg/ml)		
	Mean width of inhibition zone (mm)	MICs (μg/ml)	MBCs (μg/ml)
SL-1	16.17 ± 0.29	32	128
SL-2	10.67 ± 0.27	32	64
SL-3	16.8 ± 0.76	32	32
SL-4	10.1 ± 0.05	16	64

The mean and standard deviation (SD) reported for each microbial strain were based on three biological replicates. For MIC and MBC values, the standard deviation of a data set is zero because all of its values were identical [38].

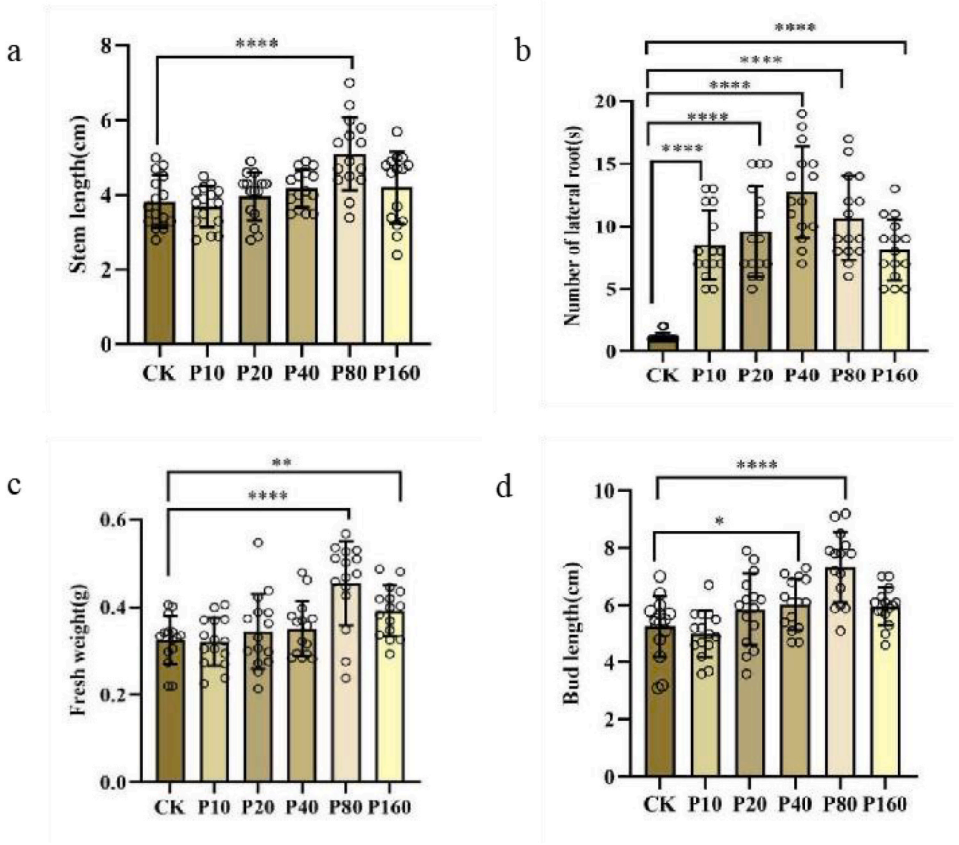

Fig. 4. Influence of varied AgNP concentrations on Safflower seed growth (a) Stem length, (b) Number of lateral roots, (c) Fresh weight, and (d) Bud length Asterisk indicates statistical significance between AgNPs treatments and control. (P10: 10 μg/mL; P20: 20 μg/mL; P40: 40 μg/mL; P80: 80 μg/mL; P160: 160 μg/mL). *, $p < 0.05$; **, $p < 0.01$; ***, $p < 0.001$; ****, $p < 0.0001$.

Different pathogenic bacteria displayed varying sensitivities to AgNPs, as evidenced by distinct inhibition zone sizes.

AgNPs influence the growth and development of higher plants [50,51]. When added to soybean, AgNPs demonstrated a concentration-dependent increase in branch and root length, leaf surface area, chlorophyll, and carbohydrate content [52]. In commercial crops, AgNPs promote adventitious bud formation, *in vitro* flowering, and fruiting. AgNPs treatment resulted in significantly longer roots in rice seedlings. *C. tinctorius*, a traditional Chinese herb known to stimulate blood circulation, relieve congestion, and reduce pain, has safflower oil with the highest linoleic acid concentration among vegetable oils, offering high nutritional value and the ability to lower serum cholesterol levels in humans [53]. In this study, 80 μg/mL of the biosynthesized AgNPs promoted safflower seed germination and seedling growth. We hypothesized that AgNPs penetrate the seed coat, facilitating seed germination. Small AgNPs, due to their size, can easily penetrate the biological barrier of the seed coat, increasing ROS accumulation [54]. This triggers stress/immune responses, induces the reprogramming of defense-related metabolites and genes, and reduces malondialdehyde and hydrogen peroxide levels in the seeds. This enhanced resistance to future abiotic and biotic stresses indirectly promotes seedling growth [55–57].

This study exclusively examined the *in vitro* antimicrobial activity of AgNPs and did not assess their efficacy in preventing diseases caused by pathogenic fungi and bacteria. Furthermore, AgNPs, when used as elicitors, can enhance various plant growth parameters, including bud and root length, leaf area, biochemical characteristics, and secondary metabolite concentrations in medicinal plants [58]. Future investigations will prioritize exploring these aspects.

5. Conclusions

This study developed a simple, environmentally friendly approach for synthesizing AgNPs using the secondary fermentation broth of the *P. polonicum* PG21 strain. The resulting AgNPs exhibited inhibitory effects on pathogenic fungal and bacterial growth, influencing seed germination and seedling growth significantly. The inhibition rate of pathogenic fungi increased proportionally with the concentration of AgNPs, particularly with EB-1, where the most effective concentration for fungal inhibition was 60 μg/mL. AgNPs exhibited varied inhibition zones for different bacteria, highlighting the distinct sensitivity of the four bacteria to AgNPs. SL-3 displayed the highest sensitivity. Conversely, SL-4 showed minimal sensitivity to AgNPs. The most effective concentration for bacterial

inhibition was determined to be 200 μg/mL. Simultaneously, the impact of AgNPs on safflower seed germination and growth was investigated. Treatment groups outperformed the control in lateral root number, stem length, fresh weight, and bud length across different AgNPs concentrations. Notably, the P80-treated group exhibited superior bud length, fresh weight, and stem length compared to other groups. These findings are pivotal for investigating the antimicrobial properties of AgNPs and determining their potential applications in agriculture.

CRediT authorship contribution statement

Yunhao Zhu: Writing – review & editing, Data curation, Conceptualization. **Xiangxiang Hu:** Writing – original draft, Investigation. **Mengyi Qiao:** Investigation, Data curation, Writing – review & editing. **Le Zhao:** Writing – review & editing. **Chengming Dong:** Writing – review & editing, Funding acquisition.

Declaration of competing interest

The authors declare that they have no known competing financial interests or personal relationships that could have appeared to influence the work reported in this paper.

Acknowledgements

The authors are thankful to Prof. Weisheng Feng for technical assistance with secondary metabolites analysis.This work was funded by the National Natural Science Foundation of China (Grant No. 81603232), The National key research and development program of China (Grant No. 2017YFC1702800). We thank Bullet Edits Limited for the linguistic editing and proofreading of the manuscript.

Appendix A. Supplementary data

Supplementary data to this article can be found online at doi:mmcdoino

References

[1] L. Zhao, J. Deng, P. Sun, J. Liu, J. Yi, N. Nakada, Z. Qiao, H. Takana, Y. Yang, Nanomaterials for treating emerging contaminants in water by adsorption and photocatalysis: systematic review and bibliometric analysis, Sci. Total Environ. 627 (2018) 1253–1263, https://doi.org/10.1016/j.scitotenv.2018.02.006.
[2] Y. Deligiannakis, Nanomaterials for environmental solar energy technologies : applications & limitations, Kona Power. Part. J 35 (2018) 14–31, https://doi.org/10.14356/kona.2018004.
[3] M. Pan, J. Yang, K. Liu, Z. Yin, T. Ma, S. Liu, L. Xu, S. Wang, Noble metal nanostructured materials for chemical and biosensing systems, Nanomaterials 10 (2020) 209, https://doi.org/10.3390/nano10020209.
[4] X. He, F. Leonard, J. Kono, Uncooled carbon nanotube photodetectors, Adv. Opt. Mater. 3 (2015) 989–1011, https://doi.org/10.1002/adom.201500237.
[5] G. Ghasemzadeh, M. Momenpour, F. Omidi, M.R. Hosseini, M. Ahani, A. Barzegari, Applications of nanomaterials in water treatment and environmental remediation, Front. Env. Sci. Eng. 8 (2014) 471–482, https://doi.org/10.1007/s11783-014-0654-0.
[6] S. Dare, J. Kharraz, A. Giwa, S.W. Hasanet, Recent applications of nanomaterials in water desalination: a critical review and future opportunities, Desalination 367 (2015) 37–48, https://doi.org/10.1016/j.desal.2015.03.030.
[7] W.S. Jiang, D. Rutherford, T. Vuong, H. Liu, Nanomaterials for treating cardiovascular diseases: a review, Bioact. Mater. 2 (2017) 185–198, https://doi.org/10.1016/j.bioactmat.2017.11.002.
[8] M.A. Hossen, S. Jean-Marie, T.P. Huong, N. Muhammad, L. Chen, G. Lakshman, C. Mumtaz, T.M. Raymood, Carbon nanoparticles functionalized with carboxylic acid improved the germination and seedling vigor in upland boreal forest species, Nanomaterials 10 (2020) 176, https://doi.org/10.3390/nano10010176.
[9] M. Rai, A.P. Ingle, S. Birla, A. Yadav, C.A.D. Santos, Strategic role of selected noble metal nanoparticles in medicine, Crit. Rev. Microbiol. 42 (2016) 696–719, https://doi.org/10.3109/1040841X.2015.1018131.
[10] X. Zhao, K. Drlica, Reactive oxygen species and the bacterial response to lethal stress, Curr. Opin. Microbiol. 21 (2014) 1–6, https://doi.org/10.1016/j.mib.2014.06.008.
[11] T.J. Berger, J.A. Spadaro, S.E. Chapin, R.O. Becker, Electrically generated silver ions: quantitative effects on bacterial and mammalian cells, Antimicrob. Agents Ch. 9 (1976) 357–358, https://doi.org/10.1128/AAC.9.2.357.
[12] J.S. Min, K.S. Kim, S.W. Kim, J.H. Jung, K. Lamsal, S.B. Kim, M. Jung, Y.S. Lee, Effects of colloidal silver nanoparticles on sclerotium-forming phytopathogenic fungi, Plant Pathology J. 25 (2009) 376–380, https://doi.org/10.5423/PPJ.2009.25.4.376.
[13] A. Byczyńska, A. Zawadzińska, P. Salachna, Silver nanoparticles preplant bulb soaking affects tulip production, Acta Agr. Scand. B-S. P. 69 (2019) 250–256, https://doi.org/10.1080/09064710.2018.1545863.
[14] P. Jadczak, D. Kulpa, M. Bihun, W. Przewodowski, Positive effect of AgNPs and AuNPs *in vitro* cultures of *Lavandula angustifolia* mill, plant cell tiss, Org 139 (2019) 191–197, https://doi.org/10.1007/s11240-019-01656-w.
[15] Z.M. Almutairi, Influence of silver nano-particles on the salt resistance of tomato (*Solanum lycopersicum L.*) during germination, Int. J. Agric. Biol. 18 (2016) 449–457, https://doi.org/10.17957/IJAB/15.0114.
[16] K. Kalimuthu, R.S. Babu, D. Venkataraman, M. Bilal, S. Gurunathanet, Biosynthesis of silver nanocrystals by *Bacillus licheniformis*, Colloid. Surface. B. 65 (2008) 150–153, https://doi.org/10.1016/j.colsurfb.2008.02.018.
[17] K. Cekuolyte, R. Gudiukaite, V. Klimkevicius, V. Mazrimaite, A. Maneikis, E. Lastauskiene, Biosynthesis of silver nanoparticles produced using *Geobacillus* spp. bacteria, Nanomaterials 13 (2023) 702, https://doi.org/10.3390/nano13040702.
[18] M. Malik, M.A. Iqbal, Y. Iqbal, M. Malik, S. Bakhsh, S. Irfan, R. Ahmad, P.V. Pham, Biosynthesis of silver nanoparticles for biomedical applications: a mini review, Inorg. Chem. Commun. 145 (2022) 109980, https://doi.org/10.1016/j.inoche.2022.109980.
[19] A. Panacek, L. Kvitek, R. Pucek, M. Kolar, R. Vecerova, N. Pizurova, V.K. Sharma, T. Nevecna, R. Zboril, Silver colloid nanoparticles: synthesis, characterization, and their antibacterial activity, J. Phys. Chem. B 110 (2006) 16248–16253, https://doi.org/10.1021/jp063826h.
[20] D. Wang, B. Xue, L. Wang, Y. Zhang, L. Liu, Y. Zhou, Fungus-mediated green synthesis of nano-silver using *Aspergillus sydowii* and its antifungal/antiproliferative activities, Sci. Rep-Uk 11 (2021) 10356, https://doi.org/10.1038/s41598-021-89854-5, 2021.

[21] C.S. Espenti, K.S.V.K. Rao, K.M. Rao, Bio-synthesis and characterization of silver nanoparticles using Terminalia chebula leaf extract and evaluation of its antimicrobial potential, Mater. Lett. 174 (2016) 129–133, https://doi.org/10.1016/j.matlet.2016.03.106.

[22] J. Asgarpanah, N. Kazemivash, Phytochemistry, pharmacology and medicinal properties of *Carthamus tinctorius* L. Chin, J. Integr. Med. 19 (2013) 153–159, https://doi.org/10.1007/s11655-013-1354-5.

[23] L. Zheng, P. Xi, J.J. SiTu, X.N. Chen, J. Li, X.D. Qin, H. Shen, C.P. Xie, First report of Phoma herbarum causing leaf spot of oil palm (*Elaeis guineensis*) in China, Plant Dis. 101 (2017) 629–630, https://doi.org/10.1094/PDIS-05-16-0692-PDN.

[24] A. Gerszberg, K. Hnatuszko-Konka, T. Kowalczyk, K.K. Andrzej, Tomato (*Solanum lycopersicum* L.) in the service of biotechnology, Plant Cell. Tiss. Org. 120 (2015) 881–902, https://doi.org/10.1007/s11240-014-0664-4.

[25] Y. Zhu, Y. Shao, L. Li, L. Zhao, M. Zhang, C. Dong, The plant growth-promoting endophytic *Fusarium oxysporum* GG22 enhances *Rehmannia glutinosa* secondary metabolites accumulation, Ind. Crop. Prod. 182 (2022) 114881, https://doi.org/10.1016/j.indcrop.2022.114881.

[26] J. Houbraken, R.A. Samson, Phylogeny of *Penicillium* and the segregation of *Trichocomaceae* into three families, Stud. Mycol. 70 (2011) 1–51, https://doi.org/10.3114/sim.2011.70.01.

[27] J. Houbraken, J.C. Frisvad, R.A. Samson, Sex in *penicillium* series roqueforti, IMA Fungus 1 (2020) 171–180, https://doi.org/10.5598/imafungus.2010.01.02.10.

[28] K. Khleifat, M. Alqaraleh, M. Al-limoun, I. Alfarrayeh, R. Khatib, H. Qaralleh, A. Ahmad, M.A. Hajleh, The ability of rhizopus stolonifer MR11 to biosynthesize silver nanoparticles in response to various culture media components and optimization of process parameters required at each stage of biosynthesis, J. Ecol. Eng. 23 (2022) 89–100, https://doi.org/10.12911/22998993/150673.

[29] W.A. Lotfy, B.M. Alkersh, S.A. Sabry, H.A. Ghozlan, Biosynthesis of silver nanoparticles by *Aspergillus terreus*: characterization, optimization, and biological activities, Front. Bioeng. Biotech. 9 (2021) 633468, https://doi.org/10.3389/fbioe.2021.633468.

[30] R. Mie, M.W. Samsudin, L.B. Din, A. Ahmad, N. Ibrahim, S.N.A. Adnan, Synthesis of silver nanoparticles with antibacterial activity using the lichen Parmotrema praesorediosum, Int. J. Nanomed. 9 (2014) 121–127, https://doi.org/10.2147/IJN.S52306.

[31] S. Bykkam, M. Ahmadipour, S. Narisngam, V.R. Kalagadda, S.C. Chidurala, Extensive studies on X-ray diffraction of green synthesized silver nanoparticles, Adv. Nanopart 4 (2015) 1–10. https://doi:10.4236/anp.2015.41001.

[32] Y. Jian, X. Chen, T. Ahmed, Q. Shang, S. Zhang, Z. Ma, Y. Yin, Toxicity and action mechanisms of silver nanoparticles against the mycotoxin-producing fungus Fusarium graminearum, J. Adv. Research. 38 (2022) 1–12, https://doi.org/10.1016/j.jare.2021.09.006.

[33] S.W. Kim, J.H. Jung, K. Lamsal, Y.S. Kim, J.S. Min, Y.S. Lee, Antifungal effects of silver nanoparticles (AgNPs) against various plant pathogenic fungi, MYCOBIOLOGY 40 (2012) 53–58, https://doi.org/10.5941/MYCO.2012.40.1.053.

[34] J. Zhang, X. Cui, M. Zhang, B. Bai, Y. Yang, S. Fan, The antibacterial mechanism of perilla rosmarinic acid, Biotechnol. Appl. Bioc. 69 (2022) 1757–1764, https://doi.org/10.1002/bab.2248.

[35] F.F. Habibah, W.O.S. Rizki, A.L. Ivansyah, D.I. Astuti, R. Hertadi, R, Green synthesis of copper ions nanoparticles Functionalized with Rhamnolipid as potential antibacterial agent for pathogenic bacteria, Heliyon (2024) e24242, https://doi.org/10.1016/j.heliyon.2024.e24242.

[36] E.D. Cavassin, L.F.P. Figueiredo, J.P. Otoch, M.M. Seckler, R. Angelo, F.F. Franco, V.S. Marangoni, V. Zucolotto, A.S.S. Levin, S.F. Costa, Comparison of methods to detect the *in vitro* activity of silver nanoparticles (AgNP) against multidrug resistant bacteria, J. Nanobiotechnol. 64 (2015) 1757–1764, https://doi.org/10.1186/s12951-015-0120-6.

[37] S. Laha, T. Subrahmanyeswari, S.K. Verma, S. N Kamble, S. Singh, S. Bhattacharyya, S. Gantait, Biogenic synthesis, characterization and application of silver nanoparticles as biostimulator for growth and rebaudioside-A production in genetically stable stevia (Stevia rebaudiana Bert.) under *in vitro* conditions, Ind. Crop. Prod. 197 (2023) 116520, https://doi.org/10.1016/j.indcrop.2023.116520.

[38] D. Garibo, H.A.B. Nuñez, J.N.D. León, E.G. Mendoza, I. Estrada, Y.T. Magaña, A.S. Arce, Green synthesis of silver nanoparticles using Lysiloma acapulcensis exhibit high-antimicrobial activity, Sci. Rep. 10 (2020) 12805, https://doi.org/10.1038/s41598-020-69606-7.

[39] N. Ilahi, A. Haleem, S. Iqbal, N. Fatima, W. Sajjad, A. Sideeq, S. Ahmed, Biosynthesis of silver nanoparticles using endophytic *Fusarium oxysporum* strain NFW16 and their *in vitro* antibacterial potential, Microsc. Res. Techniq. 85 (2022) 1568–1579, https://doi.org/10.1002/jemt.24018.

[40] H. Mistry, R. Thakor, C. Patil, J. Trivedi, H. Bariya, Biogenically proficient synthesis and characterization of silver nanoparticles employing marine procured fungi Aspergillus brunneoviolaceus along with their antibacterial and antioxidative potency, Biotechnol. Lett. 43 (2021) 307–316, https://doi.org/10.1007/s10529-020-03008-7.

[41] T. Gupta, J. Saxena, Biogenic synthesis of silver nanoparticles from Aspergillus oryzae mtcc 3107 against plant pathogenic fungi Sclerotinia sclerotiorum mtcc 8785, J. Microb. Biotec. Food 12 (2023), https://doi.org/10.55251/jmbfs.9387 e9387-e9387.

[42] N. Vigneshwaran, N.M. Ashtaputre, P.V. Varadarajan, R.P. Nachane, M. ParalikarK, R.H. Balasubramanya, Biological synthesis of silver nanoparticles using the fungus *Aspergillus flavus*, Mater. Lett. 61 (2007) 1413–1418, https://doi.org/10.1016/j.matlet.2006.07.042.

[43] N.S. Shaligram, M. Bule, R. Bhambure, R.S. Singhal, S.K. Singh, G. Szakacs, A. Pandey, Biosynthesis of silver nanoparticles using aqueous extract from the compactin producing fungal strain, Process Biochem 44 (2009) 939–943, https://doi.org/10.1016/j.procbio.2009.04.009.

[44] A. Ahmad, P. Mukherjee, S. Senapati, D. Mandal, M. Khan, R. Kumar, M. Sastry, Extracellular biosynthesis of silver nanoparticles using the fungus *Fusarium oxysporum*, Colloids. Surface. B. 28 (2003) 313–318, https://doi.org/10.1016/S0927-7765(02)00174-1.

[45] D. MubarakAli, M. Sasikala, M. Gunasekaran, N. Thajuddin, Biosynthesis and characterization of silver nanoparticles using marine cyanobacterium, Oscillatoria willei NTDM01, Dig, J. Nanomater. Biostruct. 6 (2011) 385–390, https://doi.org/10.1049/mnl.2011.0053.

[46] M. Alavi, M. Ashengroph, Mycosynthesis of AgNPs: mechanisms of nanoparticle formation and antimicrobial activities, Expert. Rev. Anti-Infe. 21 (2023) 355–363, https://doi.org/10.1080/14787210.2023.2179988.

[47] K. Manimaran, D.H.Y. Yanto, S.H. Anita, O.D. Nurhayat, K. Selvaraj, S. Basavarajappa, K. Kumarasamy, Synthesis and characterization of Hypsizygus ulmarius extract mediated silver nanoparticles (AgNPs) and test their potentiality on antimicrobial and anticancer effects, Environ. Res. 235 (2023) 116671, https://doi.org/10.1016/j.envres.2023.116671.

[48] F. Ameen, A.A. Al-Homaidan, A. Al-Sabri, A. Almansob, S. AlNAdhari, Anti-oxidant, anti-fungal and cytotoxic effects of silver nanoparticles synthesized using marine fungus Cladosporium halotolerans, Appl. Nanosci. 13 (2023) 623–631, https://doi.org/10.1007/s13204-021-01874-9.

[49] R. Singh, A.K. Gupta, V.Y. Patade, G. Balakrishna, H.K. Pandey, A. Singh, Synthesis of silver nanoparticles using extract of Ocimum kilimandscharicum and its antimicrobial activity against plant pathogens, SN Appl. Sci. 1 (2019) 1652, https://doi.org/10.1007/s42452-019-1703-x.

[50] S. Khan, M. Zahoor, R.S. Khan, M. Ikram, N.U. Islam, The impact of silver nanoparticles on the growth of plants: the agriculture applications, Heliyon 9 (2023) e16928, https://doi.org/10.1016/j.heliyon.2023.e16928.

[51] M. Ansari, S. Ahmed, A. Abbasi, N.A. Hamad, H.M. Ali, M.T. Khan, Q.U. Zaman, Green synthesized silver nanoparticles: a novel approach for the enhanced growth and yield of tomato against early blight disease, Microorganisms 11 (886) (2023) 11040886, https://doi.org/10.3390/microorganisms.

[52] J. Jampílek, K. Kráľová, Nanoparticles for improving and augmenting plant functions, in: Advances in Nano-Fertilizers and Nano-Pesticides in Agriculture, 2021, pp. 171–227.

[53] L. Abou, L.G. Angelini, S. Tavarini, Genotype and SeasonalVariation affect yield and oil quality of safflower (*Carthamus tinctorius* L.) under mediterranean conditions, Agronomy 12 (2022) 122, https://doi.org/10.3390/agronomy12010122.

[54] S. Golinejad, M.H. Mirjalili, H. Rezadoost, M. Ghorbanpour, Molecular, biochemical, and metabolic changes induced by gold nanoparticles in Taxus baccata L. cell culture, Ind. Crop. Prod. 192 (2023) (2023) 115988, https://doi.org/10.1016/j.indcrop.2022.115988.

[55] L. Zheng, F. Hong, S. Lu, C. Liu, Effect of nano-TiO_2 on strength of naturally aged seeds and growth of spinach, Biol. Trace Elem. Res. 104 (2005) 83–91, https://doi.org/10.1385/BTER:104:1:083.

[56] F. Mirzajani, H. Askari, S. Hamzelou, M. Farzaneh, A. Ghassempou, Effect of silver nanoparticles on *Oryza sativa* L. and its rhizosphere bacteria, Ecotox. Environ. Safe. 88 (2013) 48–54, https://doi.org/10.1016/j.ecoenv.2012.10.018.
[57] A.K.S. Mohamed, M.F. Qayyum, A.M. Abdel-Hadi, R.A. Rehman, S. Ali, M. Rizwan, Interactive effect of salinity and silver nanoparticles on photosynthetic and biochemical parameters of wheat, Arch. Agron Soil Sci. 63 (2017) 1736–1747, https://doi.org/10.1080/03650340.2017.1300256.
[58] S. Mahajan, J. Kadam, P. Dhawal, S. Barve, S. Kakodkar, Application of silver nanoparticles in in-vitro plant growth and metabolite production: revisiting its scope and feasibility, Plant Cell Tiss. Org. (2022) 15–39, https://doi.org/10.1007/s11240-022-02249-w.